

SUPPLEMENT

Interseismic Coupling and Slow Slip Events on the Cascadia Megathrust

Pure and Applied Geophysics

Sylvain Michel^{1,2}, Adriano Gualandi^{2,3}, Jean-Philippe Avouac²

¹ University of Cambridge, Department of Earth Sciences, Bullard Laboratories, Madingley Road,
Cambridge, Cambridgeshire, CB3 0EZ, UK

² California Institute of Technology, Department of Geology and Planetary Sciences, 1200 E California
Blvd, Pasadena, CA, 91125, USA

³ Jet Propulsion Laboratory, California Institute of Technology, 4800 Oak Grove Dr, Pasadena, CA,
91109, USA

Sylvain Michel: sylvain_michel@live.fr (Corresponding author)

Adriano Gualandi : adriano.geolandi@gmail.com

Jean-Philippe Avouac : avouac@gps.caltech.edu

S.1. Trajectory Model

For every position time series $x_j(t)$, with $j = 1, \dots, M$, we perform a least square minimization to find the optimal parameters of the following model:

$$x_j(t) = x_{0j} + v_{0j}t + A_{1j}^{sin} \sin(f_1 t + \phi_{1j}) + A_{2j}^{sin} \sin(f_2 t + \phi_{2j}) + \sum_k^{N_{instr}} A_{jk}^{instr} H(t - t_k) + \sum_k^{N_{eq}} H(t - t_k) \left[A_{jk}^{co} + A_{jk}^{post} \left(1 - \exp(-(t - t_k)/\tau_{jk}) \right) \right]. \quad (\text{Eq. S1})$$

The model includes a linear trend with intercept x_{0j} and slope v_{0j} , two seasonal signals with fixed half-year ($1/f_1$) and one year ($1/f_2$) periods defined by the amplitudes A_{*j}^{sin} and phases ϕ_{*j} , instrumental offsets, co-seismic offsets and post-seismic displacement. The list of instrumental offsets is taken from the NGL database, and the offsets are described by the parameters A_{jk}^{instr} . The list of earthquakes potentially affecting a certain station is a reduced version of that present in the NGL database. In our study, a potential step record appears when the epicentral distance is less than $10^{(M/3)}$, where M is the earthquake magnitude, instead of $10^{(M/2 - 0.8)}$ originally used by NGL. The number of effective events is thus 11 (Table S1), and the co-seismic steps are described by the parameters A_{jk}^{co} . Finally, the post-seismic deformation is approximated with an exponential decay function for which the amplitude A_{jk}^{post} and the relaxation time τ_{jk} are estimated. We fix the post-seismic amplitude for the M_w 5.9 2010/02/04 event to 0 because it was preceded by a M_w 6.5, and the estimation of multiple exponential decays seems to compromise the slope of the linear trend. For the same reason, we impose an upper bound of 3 yr on the relaxation time τ_{jk} for all the listed events.

Table S1. Selection of stations for which we correct for postseismic deformation.

| Section | Stations |
|----------------|--|
| North | HOLB, BCPH, BCOV, ELIZ, WOST, NTKA, GLDR, TFNO, QUAD, UCLU, BAMF, PTAL |
| South | All stations within this section |

Table S2. Correlation between GRACE-derived and GPS derived seasonal components.

| vbICA Components | GPS 1 | GPS 2 | GPS 3 | GPS 4 |
|-------------------------|--------------|--------------|--------------|--------------|
| GRACE 1 | 0.6736 | 0.1299 | 0.4053 | 0.4732 |
| GRACE 2 | 0.2217 | 0.2514 | 0.0438 | 0.4161 |
| GRACE 3 | 0.1815 | 0.1964 | 0.2732 | 0.4965 |

Table S3. Node coordinates of the representative line of the average along-strike location of SSEs.

| Node # | Longitude | Latitude |
|---------------|------------------|-----------------|
| 1 | -125.805 | 49.3502 |
| 2 | -125.13 | 49.0498 |
| 3 | -124.464 | 48.7454 |
| 4 | -123.968 | 48.52 |
| 5 | -123.639 | 48.2797 |
| 6 | -123.311 | 47.9643 |
| 7 | -123.144 | 47.4876 |
| 8 | -123.2 | 47.0 |
| 9 | -123.291 | 46.8491 |
| 10 | -123.277 | 46.0523 |
| 11 | -123.416 | 45.2541 |
| 12 | -123.551 | 44.4556 |
| 13 | -123.545 | 44.1369 |
| 14 | -123.676 | 43.3381 |
| 15 | -123.656 | 42.3816 |
| 16 | -123.205 | 41.2694 |
| 17 | -122.83 | 40.4742 |
| 18 | -122.628 | 39.6769 |

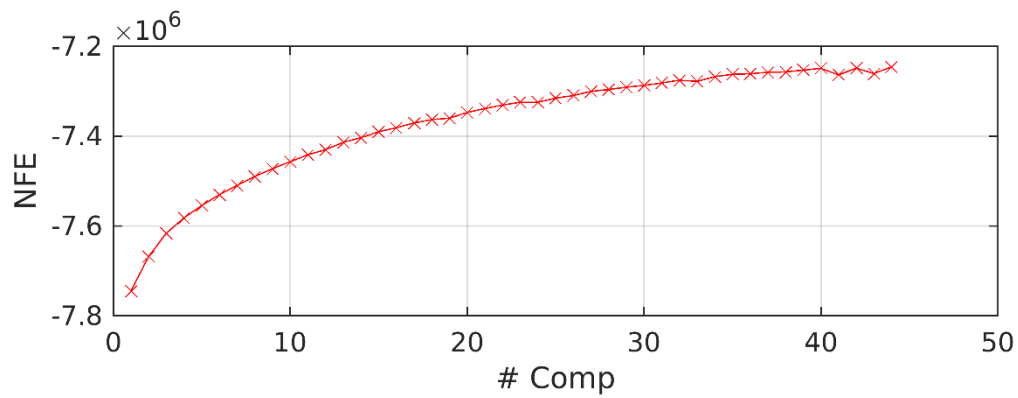


Figure S1. NFE evolution as a function of the total number of vbICA components. The curve decreases for the first time passing from 32 to 33 components. We thus selected 32 components as our final number of components.

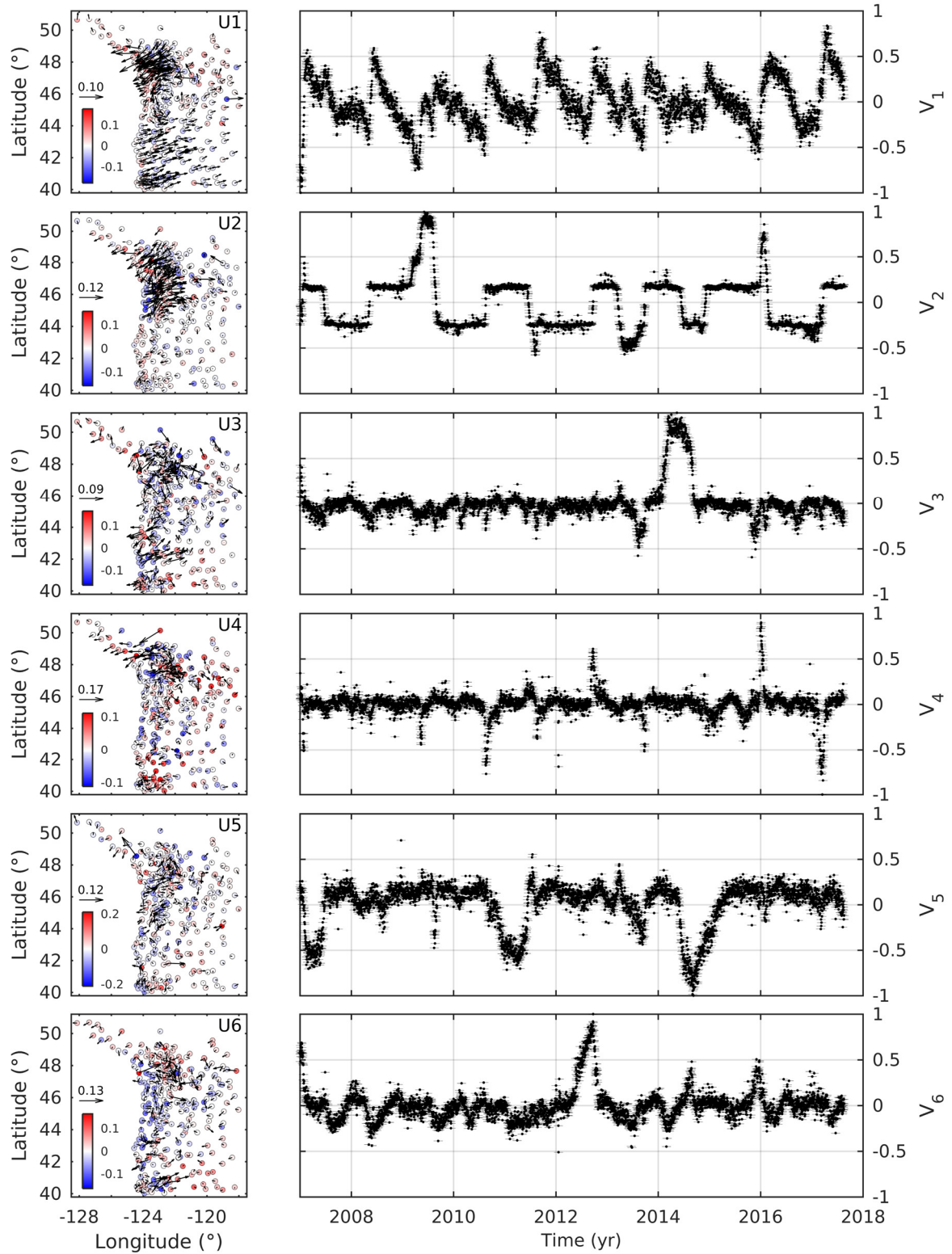


Figure S2. Spatial pattern and temporal evolution of each 32 components of Cascadia (section 3.1.4). Left column panels indicate the components spatial pattern (matrix U). The arrows and the coloured dots indicate horizontal and vertical motion, respectively. Right column panels indicate the components temporal evolution (matrix V). We consider component 1 to 15 to be related to SSE, 16 and 25 to be noise and 26 to 32 to be a local effects.

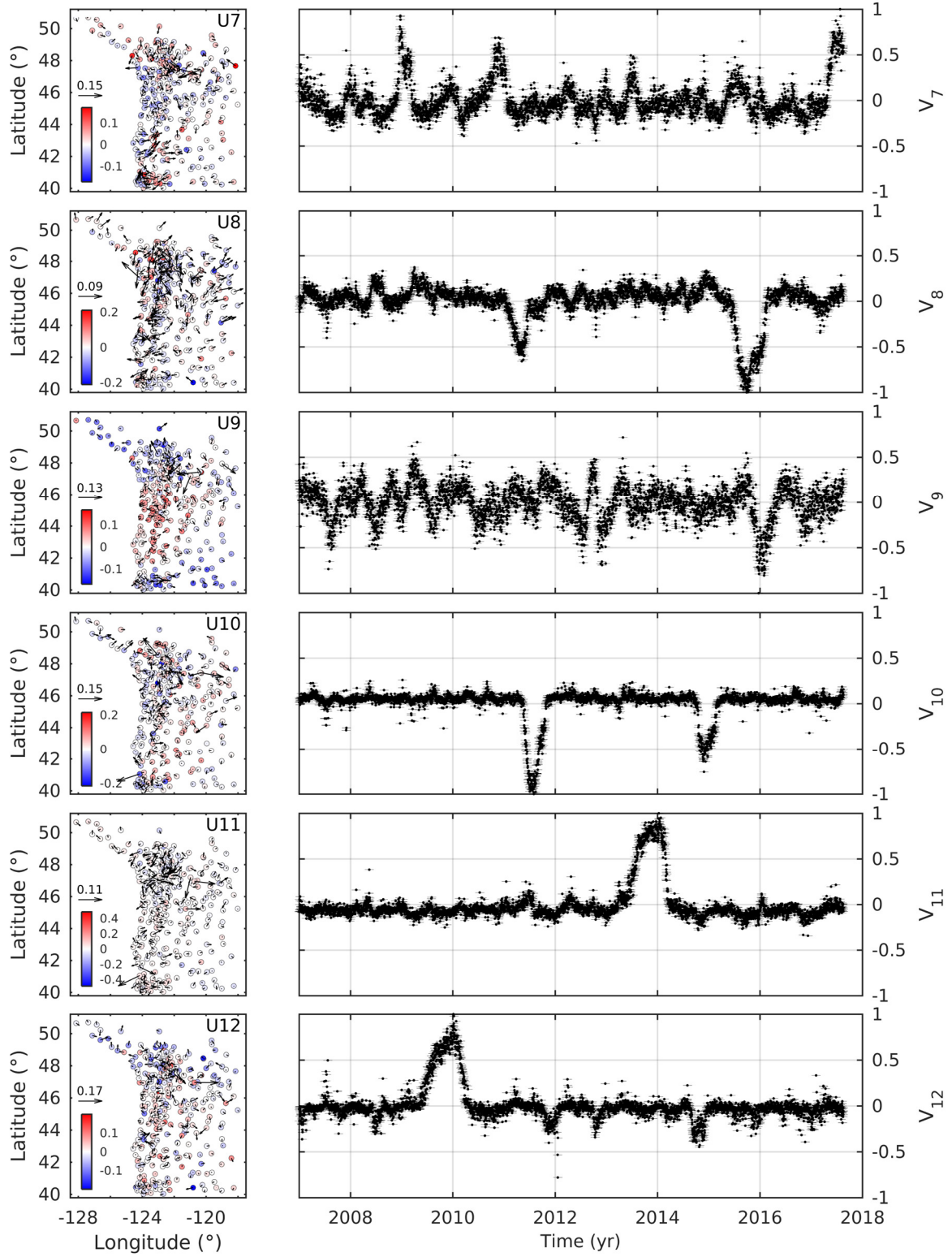


Figure S2. (Continued)

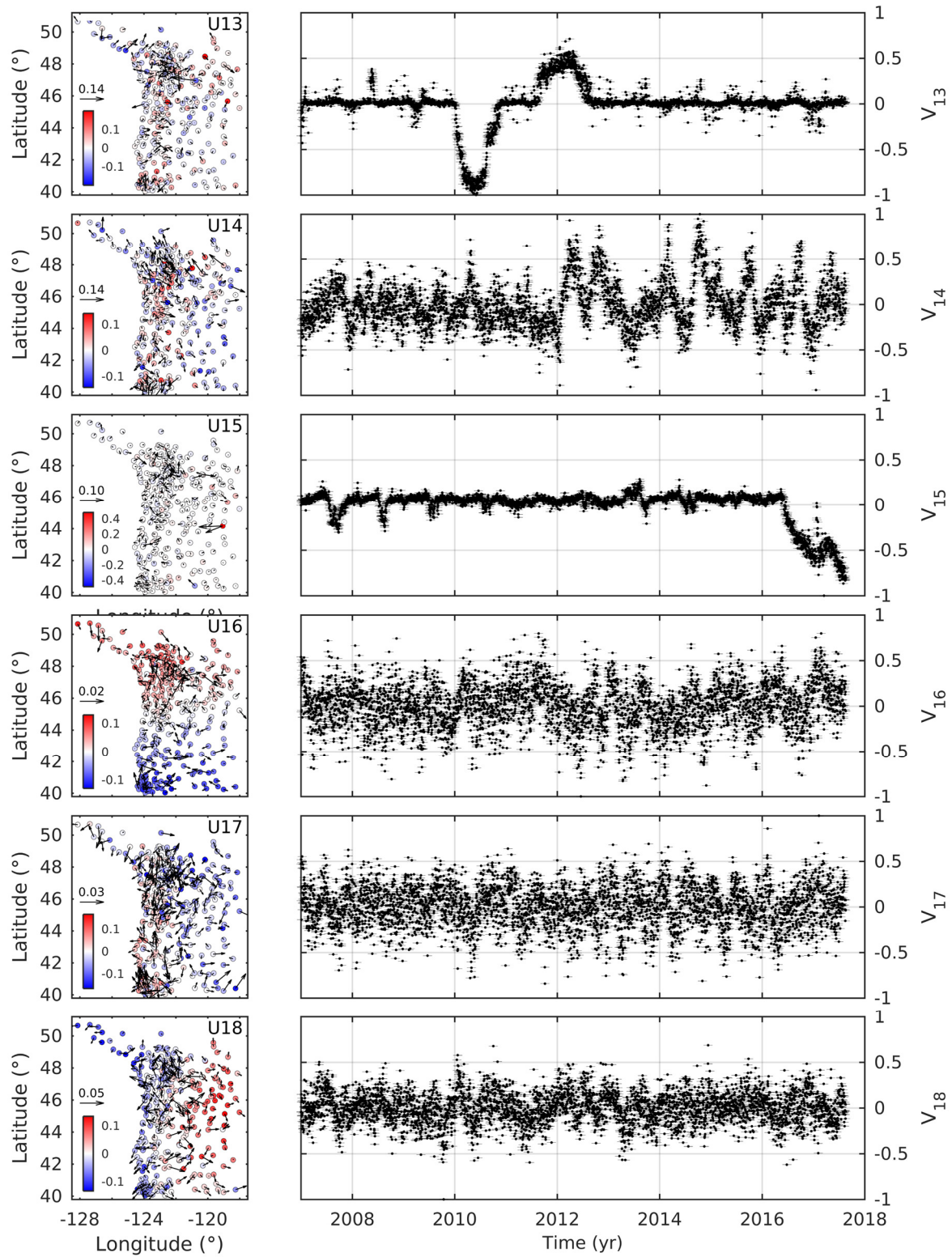


Figure S2. (Continued)

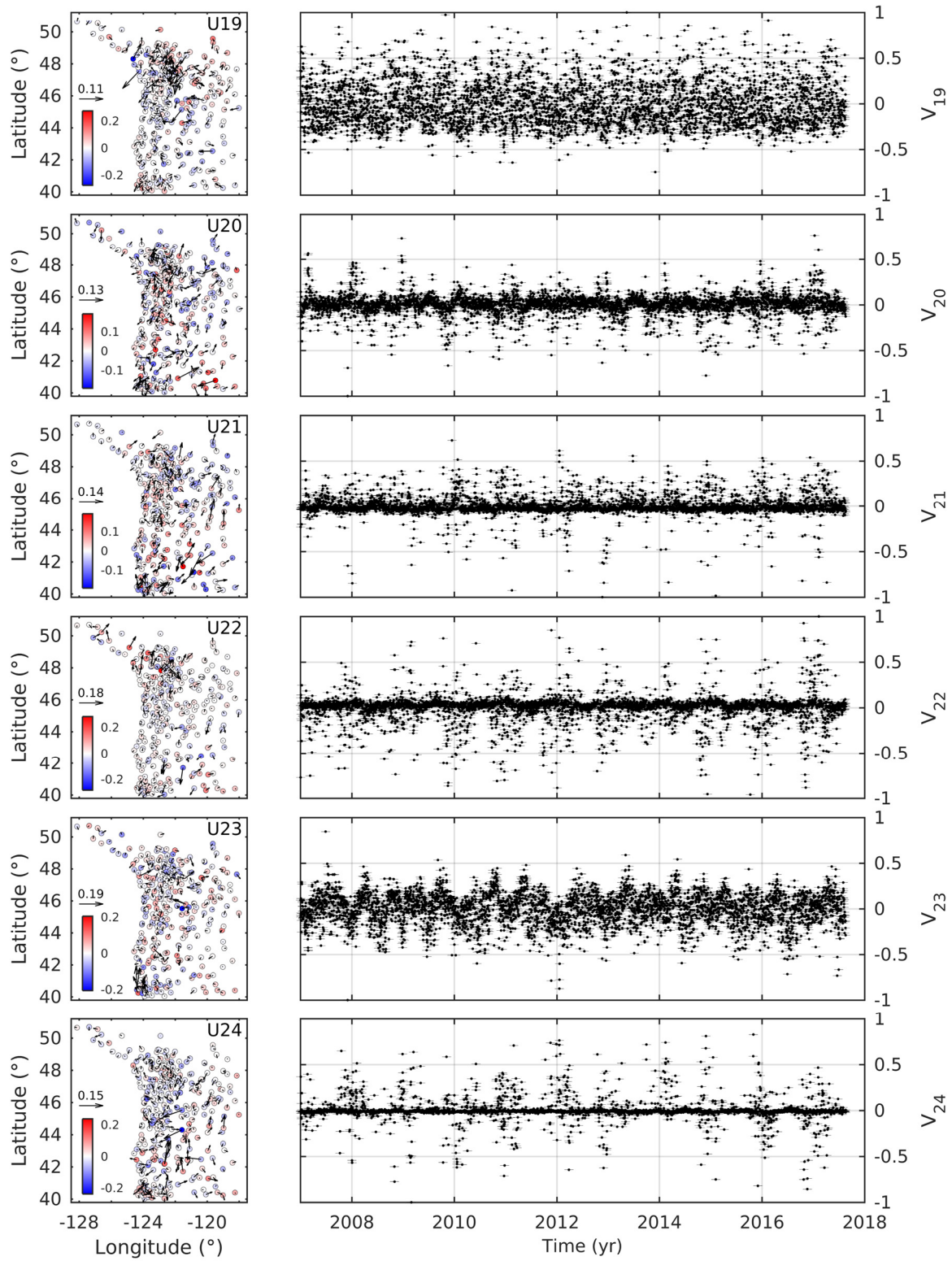


Figure S2. (Continued)

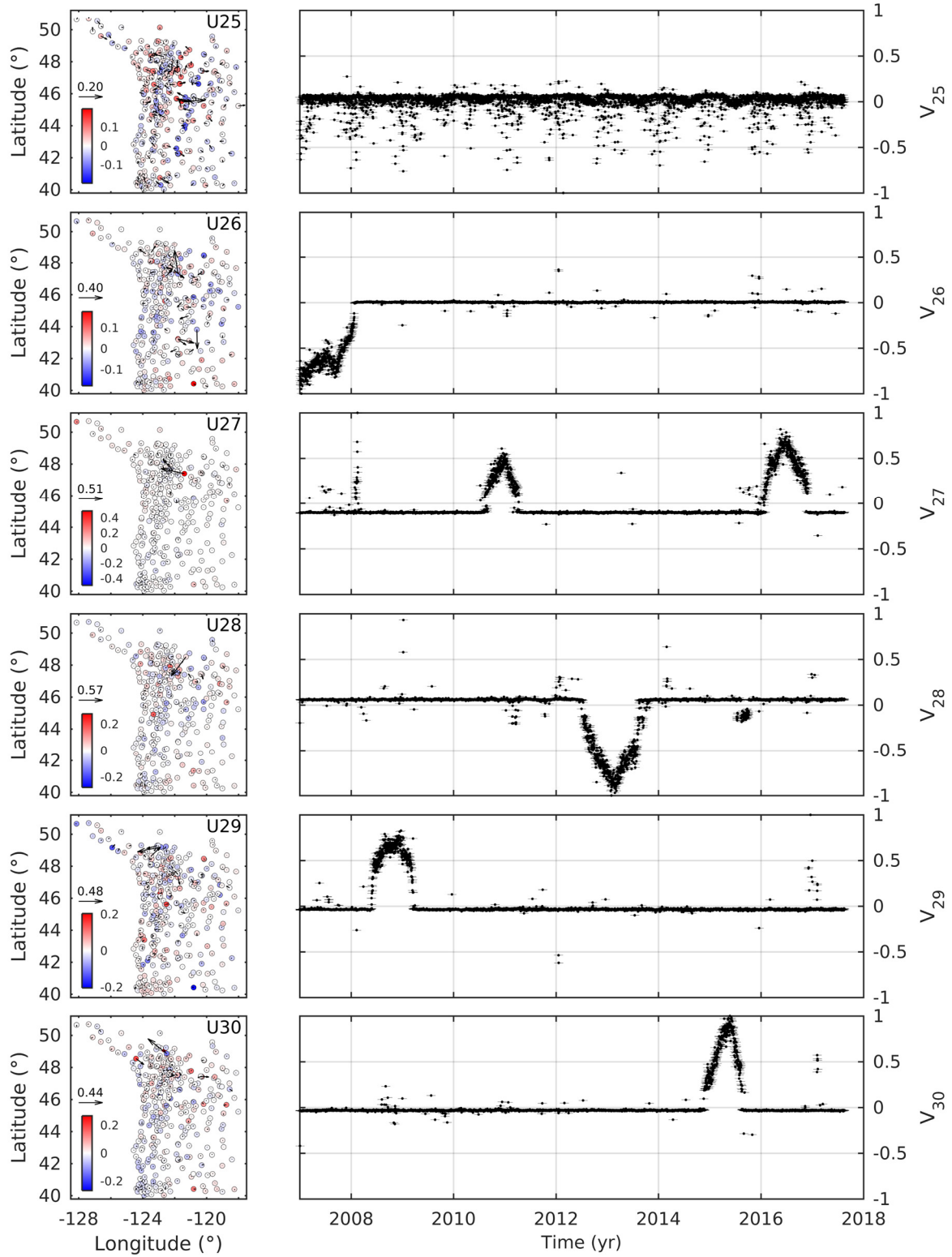


Figure S2. (Continued)

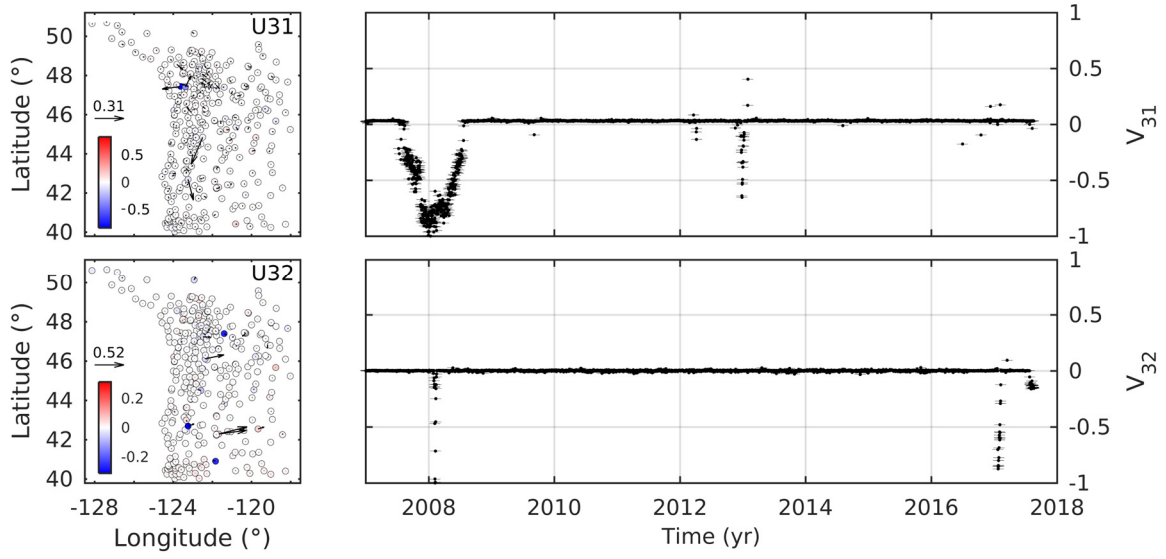


Figure S2. (Continued)

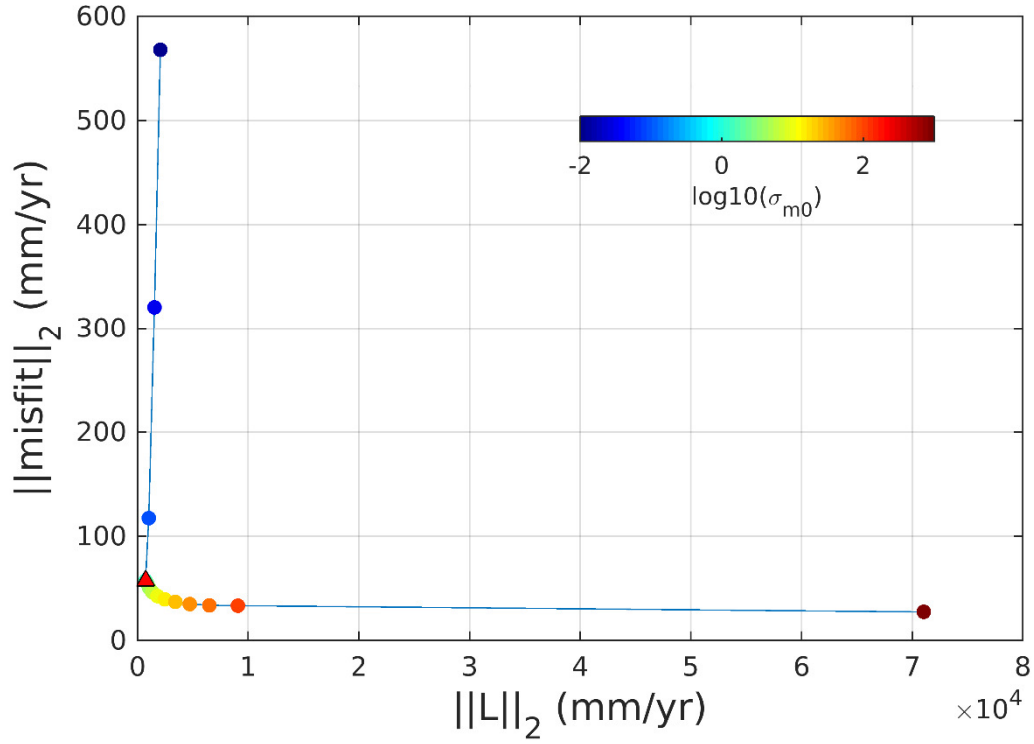


Figure S3. L-curve plot for the coupling map. On the x-axis the L_2 norm of the model obtained from the inversion of the linear system $U = GL$, where G is the matrix containing the Green's functions; on the y-axis the L_2 norm of the misfit between the spatial distribution of the inverted IC and the predicted value from the model. The colour scale indicates the values of σ_0 , ranging from 10^{-2} to 10^3 . The red triangle indicates the selected value for the inversion, corresponding to $\sigma_0 = 10^{-0.1}$. All the calculations have been performed with a fix correlation distance, $\lambda = 15.154$ km. Fixed rake constraints have been imposed using the block model plate rate directions from Schmalz et al. (2014). No positivity constraints have been imposed.

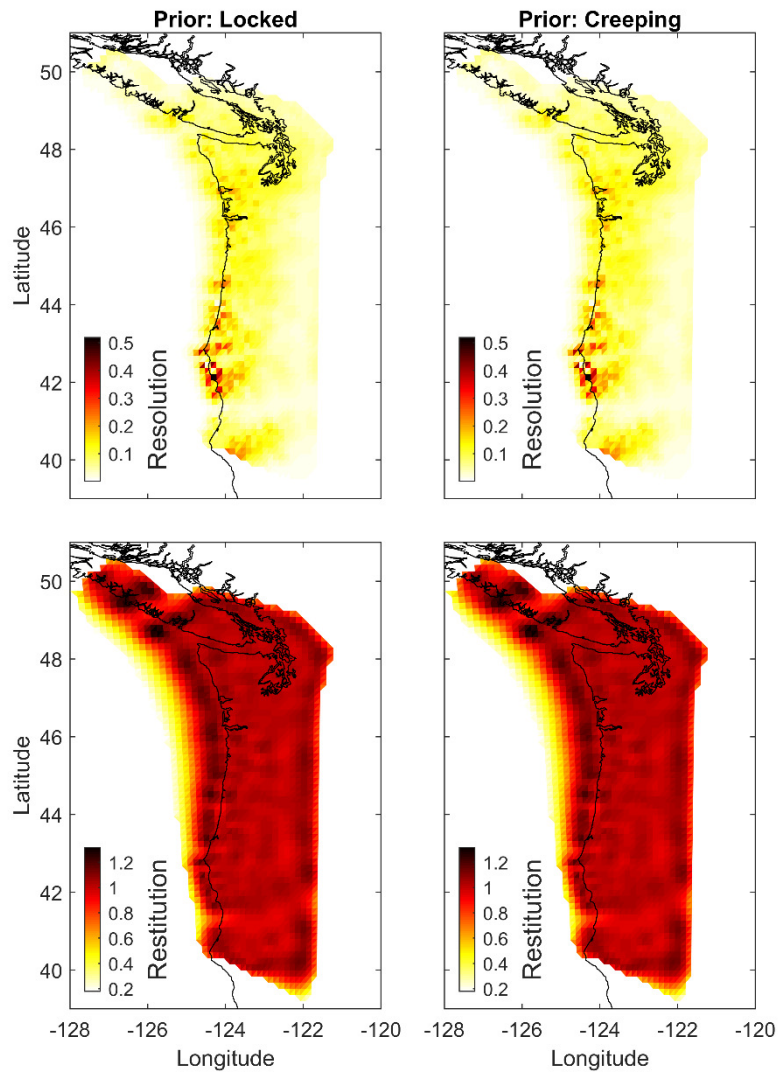


Figure S4. Resolution and restitution maps of the coupling inversions for both the locked (a,c) and creeping (b,d) *a priori* cases.

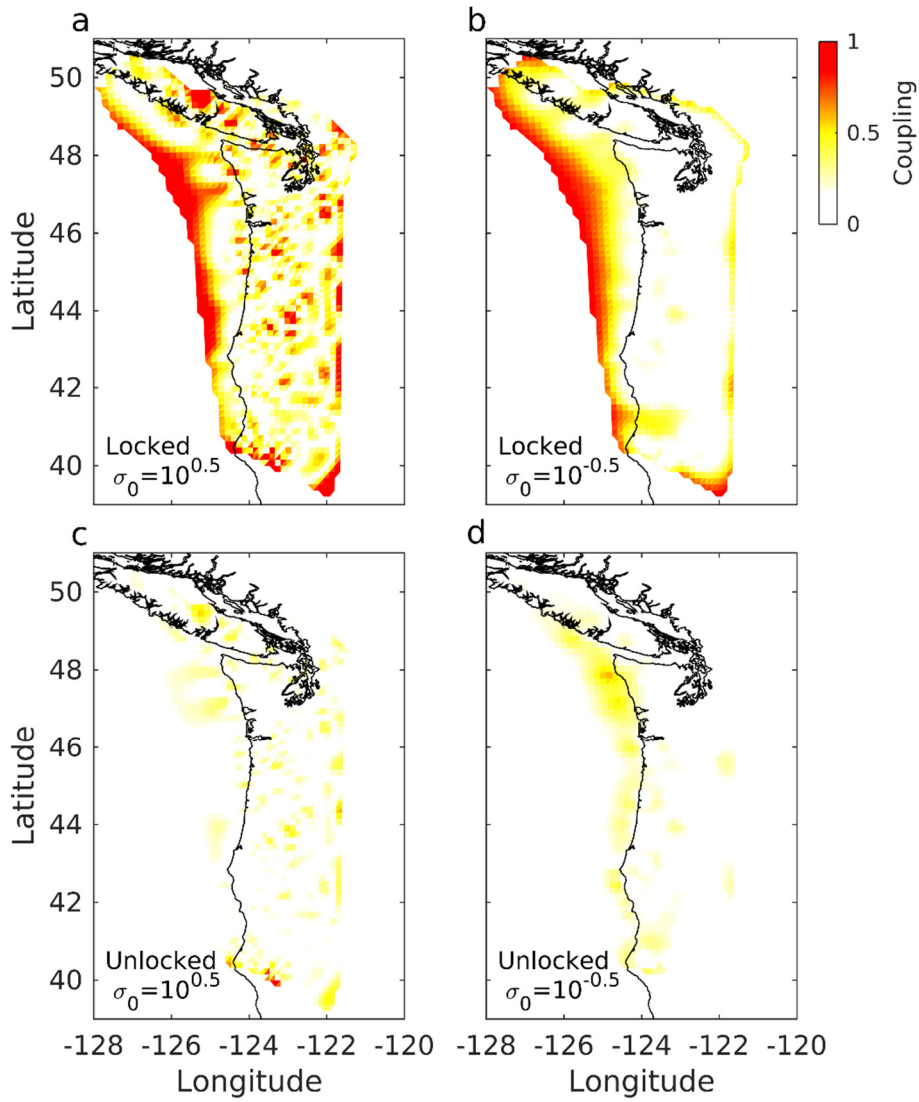


Figure S5. Coupling inversion sensitivity to σ_0 . (a) and (b) show the results for inversions using a locked fault a priori and taking $\sigma_0=10^{0.5}$ and $\sigma_0=10^{-0.5}$, respectively. (c) and (d) show the results for inversions using a creeping fault a priori and taking $\sigma_0=10^{0.5}$ and $\sigma_0=10^{-0.5}$, respectively.

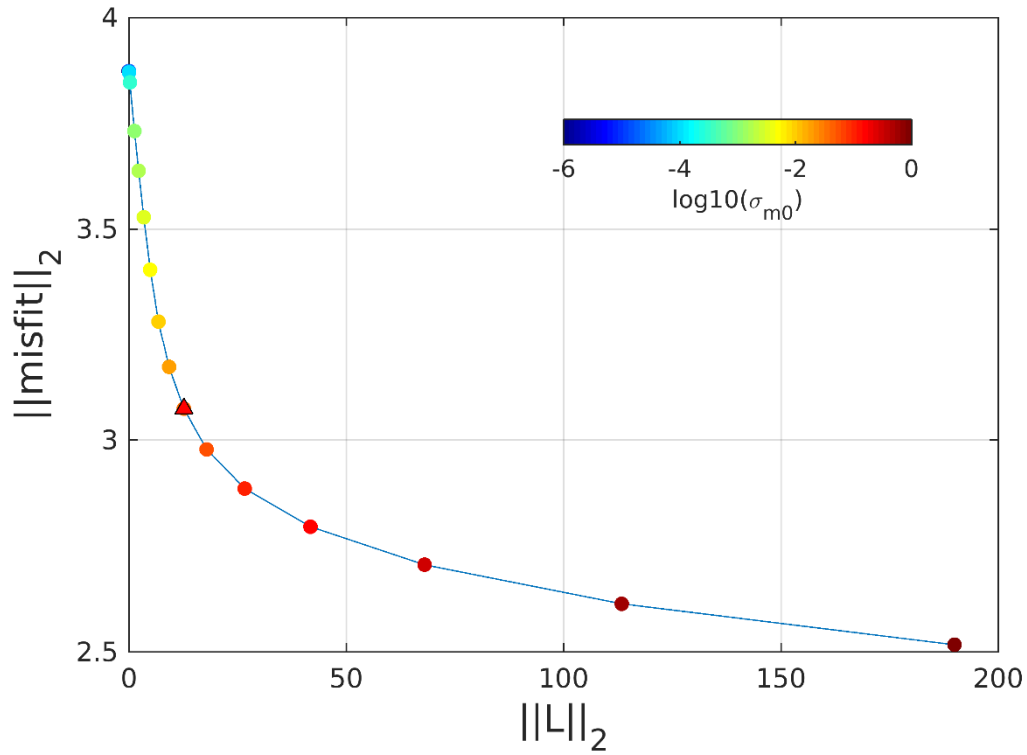


Figure S6. L-curve plot for the SSEs kinematics. On the x-axis the L_2 norm of the model obtained from the inversion of the linear system $U_{IC} = GL$, where G is the matrix containing the Green's functions; on the y-axis the L_2 norm of the misfit between the spatial distribution of the inverted IC and the predicted value from the model. Both quantities are non-dimensional. The colour scale indicates the values of σ_0 , ranging from 10^{-6} to 1. The red triangle indicates the selected value for the inversion, corresponding to $\sigma_0 = 10^{-1.5}$. All the calculations have been performed with a fix correlation distance, $\lambda = 15.154$ km. No positivity or fixed rake constraints have been imposed.

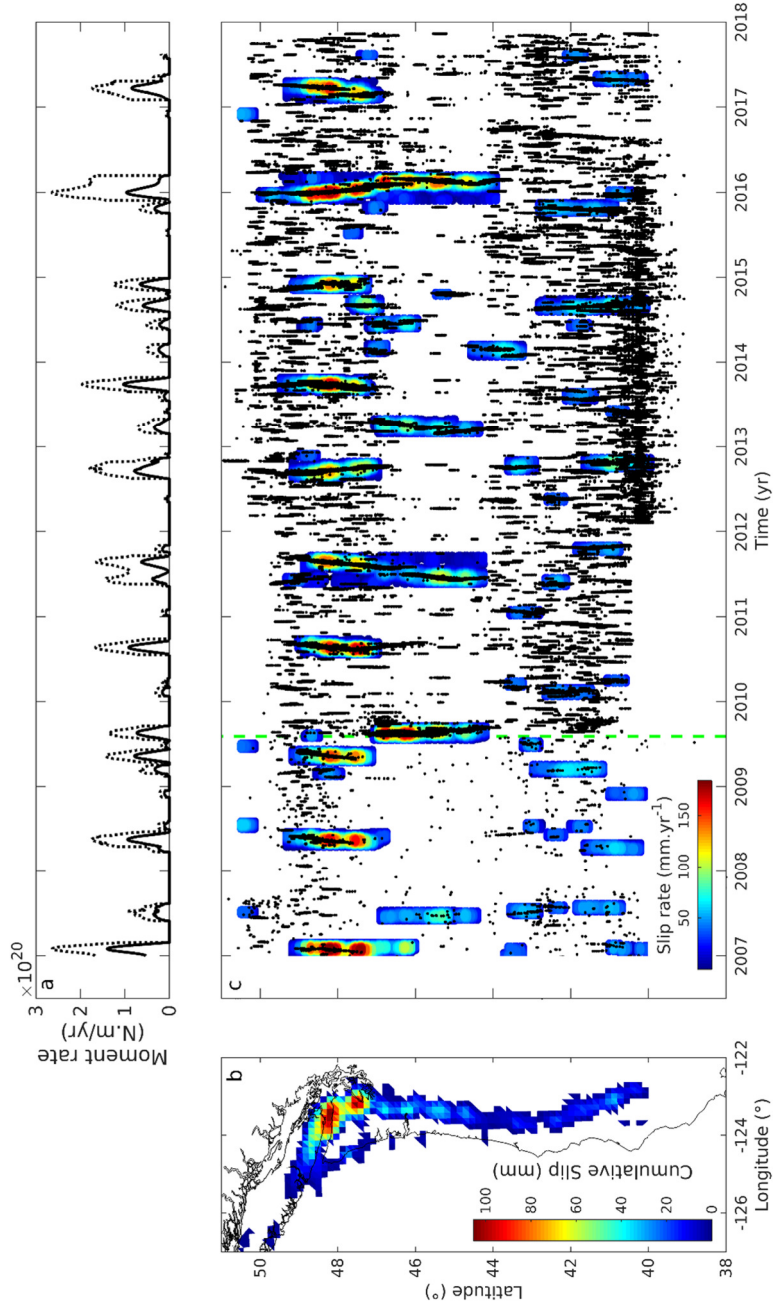


Figure S7. (a) Combined moment rate functions of all the 81 detected SSEs using $V_{\text{thresh}} = -35$ mm/yr. The continuous and dashed black lines correspond to the moment rate taking and without taking into account interseismic loading during SSEs, respectively. To place an upper bound on the moment release during SSEs the dashed lines are calculated by comparison with the moment deficit that would have accrued during each SSE had the fault remained fully locked. Those moment rate functions are based on the low-pass filtered δ_{deficit} with the passband at 21 days^{-1} (b) SSEs cumulative slip. (c) Occurrence of SSEs (colour shading) as a function of time. The black dots indicate tremors. The catalogue from Ide (2012) is used until 2009.595 (green dashed line), the catalogue from PNSN is used thereafter.

Movie S1. *The middle-left panel shows the moment rate deficit spatio-temporal evolution in respect to the long term interseismic loading. SSEs correspond to negative slip deficit rate (in blue). Tremors are indicated as black dots. The two triangles, in the north and center of Cascadia, correspond to the location for which we show the slip deficit in the top and bottom panel, respectively. The middle-right panel shows the coupling map (white to red shading) and the tremors location (black dots). The black thin lines indicate the coast. The black thick line indicates the trench location. Movie available on (<ftp://ftp.gps.caltech.edu/pub/smichel/>).*

Movie S2 to S4. *Inversion regularization sensitivity test for the SSEs kinematic model. The movies show the moment rate deficit spatio-temporal evolution of event 54 in respect to the long term interseismic loading using $\sigma_0=10^{-1}$ (Movie S2), $\sigma_0=10^{-1.5}$ (Movie S3) and $\sigma_0=10^{-2}$ (Movie S4) for the inversion regularization. SSEs correspond to negative slip deficit rate (in blue). $\sigma_0=10^{-1.5}$ is the selected value used also in Movie S1.*